Universal Quantum Optimization with Cold Atoms in an Optical Cavity

Meng Ye,[1,2,§] Ye Tian,[3,4,5,§] Jian Lin,[1] Yuchen Luo,[1,2] Jiaqi You,[3,4,5] Jiazhong Hu,[3,4,5] Wenjun Zhang,[3,4,5,*] Wenlan Chen,[3,4,5,†] and Xiaopeng Li[1,2,6,7,8,‡]

[1]*State Key Laboratory of Surface Physics, Key Laboratory of Micro and Nano Photonic Structures (MOE), and Department of Physics, Fudan University, Shanghai 200433, China*
[2]*Shanghai Qi Zhi Institute, AI Tower, Xuhui District, Shanghai 200232, China*
[3]*Department of Physics and State Key Laboratory of Low Dimensional Quantum Physics, Tsinghua University, Beijing 100084, China*
[4]*Frontier Science Center for Quantum Information, Beijing 100084, China*
[5]*Collaborative Innovation Center of Quantum Matter, Beijing 100084, China*
[6]*Institute of Nanoelectronics and Quantum Computing, Fudan University, Shanghai 200433, China*
[7]*Shanghai Artificial Intelligence Laboratory, Shanghai 200232, China*
[8]*Shanghai Research Center for Quantum Sciences, Shanghai 201315, China*

(Received 14 June 2023; accepted 15 August 2023; published 5 September 2023)

Cold atoms in an optical cavity have been widely used for quantum simulations of many-body physics, where the quantum control capability has been advancing rapidly in recent years. Here, we show the atom cavity system is universal for quantum optimization with arbitrary connectivity. We consider a single-mode cavity and develop a Raman coupling scheme by which the engineered quantum Hamiltonian for atoms directly encodes number partition problems. The programmability is introduced by placing the atoms at different positions in the cavity with optical tweezers. The number partition problem solution is encoded in the ground state of atomic qubits coupled through a photonic cavity mode, which can be reached by adiabatic quantum computing. We construct an explicit mapping for the 3-SAT and vertex cover problems to be efficiently encoded by the cavity system, which costs linear overhead in the number of atomic qubits. The atom cavity encoding is further extended to quadratic unconstrained binary optimization problems. The encoding protocol is optimal in the cost of atom number scaling with the number of binary degrees of freedom of the computation problem. Our theory implies the atom cavity system is a promising quantum optimization platform searching for practical quantum advantage.

DOI: 10.1103/PhysRevLett.131.103601

Introduction.—Quantum optimization aims at utilizing quantum fluctuations to solve difficult binary optimization problems. The idea is to encode the computation solution into the ground state of certain programmable quantum many-body Hamiltonian systems. Their ground states can be prepared using quantum adiabatic or variational principles, for example with adiabatic quantum computing (AQC) [1] or quantum approximate optimization algorithms [2]. It has wide applications that include protein folding [3], simulating molecular dynamics [4], and modeling wireless communication networks [5]. While quantum optimization may not solve NP-complete or NP-hard problems at polynomial costs, it is widely expected to exhibit significant quantum speedup over classical computing [6,7], and recent studies have shown the quantum dynamics are less vulnerable than classical searching algorithms to trapping at local minima, a standard obstacle for finding the optimal solution [8,9]. Quantum optimization protocols could benefit from even more drastic quantum speedup with machine learning based quantum algorithm configuration [10–13].

A fascinating route to implement quantum optimization has been provided by Rydberg atom arrays [14]. This atomic system naturally encodes maximum independent set problems on unit disk graphs [5]. A quantum wiring approach has been developed to mediate arbitrary connectivity, which makes the Rydberg atomic system a generic quadratic unconstrained binary optimization (QUBO) solver despite its finite interaction range [15,16]. Tremendous research efforts have been devoted to this system in recent years with remarkable progress accomplished [8,17–21]. The Rydberg system has become a prominent platform to achieve quantum advantage in practical applications [8,15,16,19,20]. However, one key limitation of this system is its quantum coherence time for the encoding Rydberg qubits involves highly excited atomic states, whose quantum coherence is fundamentally affected by blackbody radiation [22] and electromagnetic noise [23].

In this Letter, we consider a system of cold atoms in an optical cavity, whose experimental technology has been advancing rapidly in recent years [24–30], and develop a novel quantum optimization scheme for generic QUBO

problems with arbitrary connectivity using atomic ground states. The long-range atomic interactions mediated by cavity photons in this system naturally encode number partition problems (NPPs), having direct applications in multiprocessor scheduling of parallel computations and large scale truck delivery management [31]. Introducing a series of auxiliary squarefree integers, we show that 3-SAT and vertex cover problems can be efficiently encoded by the atom cavity system, where the cost of atom number scales *linearly* with number of binary degrees of freedom of the computation problem, in contrast to the *quadratic* scaling in the corresponding Rydberg encoding [15,16]. Based on this scheme, we construct an encoding scheme where QUBO problems with *arbitrary* connectivity are mapped to the atom cavity system. The overhead in the cost of atom number in representing QUBO problems has a quadratic scaling in our scheme, which is already optimal. With our theory, the atom cavity system has a potential to become a universal quantum optimization platform to demonstrate practical quantum advantage.

Solving NPPs by cold atoms in an optical cavity.—Given a set of n positive integers, $\mathcal{S} = \{p_1, p_2, \ldots, p_n\}$, NPP is to divide the set into two subsets A and $\bar{A}$ in order to minimize the imbalance $I = |\sum_{i\in A} p_i - \sum_{j\in\bar{A}} p_j|$. In order to map this computation problem to a quantum system, we rescale the integers in $\mathcal{S}$ by their maximum $p_{\max}$, and introduce $\lambda_j = p_j/p_{\max}$. The solution to NPP corresponds to the ground state of an Ising Hamiltonian,

$$\hat{H}_{\mathrm{NPP}} = \left(\sum_{i=1}^{n} \lambda_i \hat{\sigma}_i^x\right)^2, \tag{1}$$

where $\hat{\sigma}_i^x$ is the Pauli-x matrix for the ith qubit. The measurement of $\hat{\sigma}_x^i$ being positive (negative) encodes the ith integer, p_i, given to A ($\bar{A}$). The physical implementation requires the coupling between two qubits, say as labeled by i and j, to be $\lambda_i\lambda_j$, which is nonlocal.

The required Hamiltonian $\hat{H}_{\mathrm{NPP}}$ with nonlocality has natural realization with atoms interacting with cavity photons. The key idea is to utilize a cavity-mediated four-photon process to realize the desired interactions in Eq. (1). We consider N three-level atoms in a high-finesse optical cavity (Fig. 1). The qubit is encoded by the two ground states $|\uparrow\rangle$ and $|\downarrow\rangle$ with an intrinsic energy splitting $\hbar\Delta_F$. Both ground states are coupled to the excited state $|e\rangle$ by the cavity photons $\hbar\omega$, with detunings of $\Delta + \Delta_F$ and Δ, respectively. The atoms are individually trapped by optical

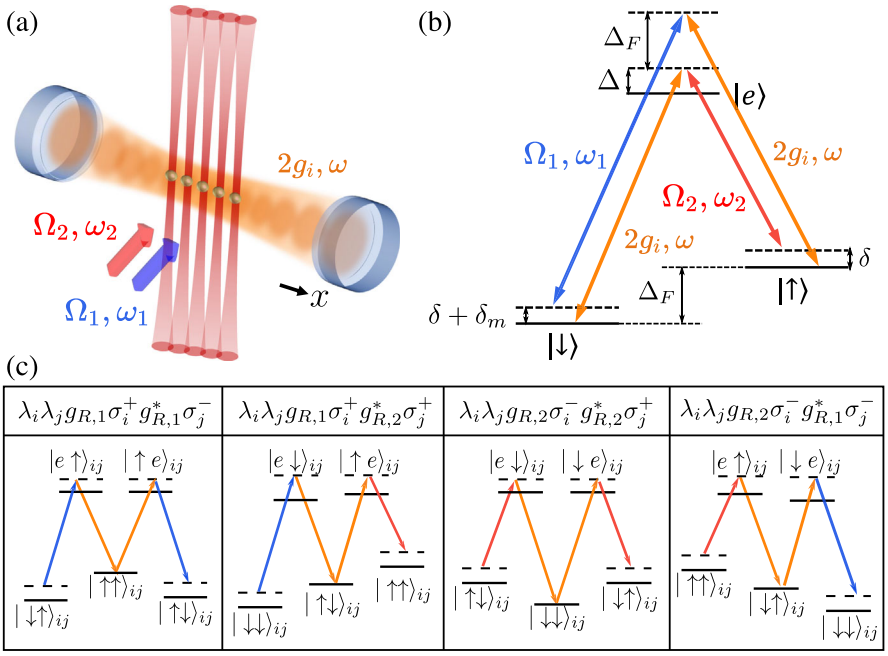

FIG. 1. Cavity QED setup for solving number partition problem. (a) Atoms are coupled to a high-finesse optical cavity. The single-photon Rabi frequency $2g_i$ for the ith atom is individually programmable by controlling the position of the atom with an optical tweezer. The atoms are illuminated by two additional beams, which are in a plane transverse to cavity axis, to generate the two Raman couplings. (b) The atomic level diagram. The qubit levels $|\uparrow\rangle$ and $|\downarrow\rangle$ are coupled to $|e\rangle$ by the same cavity mode with detunings $\Delta + \Delta_F$ and Δ, respectively. By applying two coupling beams Ω_1, Ω_2, and setting their detunings as $\Omega_1/\Omega_2 = (\Delta + \Delta_F)/\Delta$, we construct two Raman processes that couple $|\uparrow\rangle$ to $|\downarrow\rangle$ with equal two-photon Rabi frequencies g_R. The detuning δ is chosen to be much larger than g_R to suppress transitions generating multiple cavity photons. As we tune δ_m to 0, the four-photon processes become resonant. (c) Diagram of the resonant four-photon processes. These consist of two Raman processes with opposite detuning, and correspond to $\hat{\sigma}_i^+\hat{\sigma}_j^+$, $\hat{\sigma}_i^-\hat{\sigma}_j^-$, $\hat{\sigma}_i^+\hat{\sigma}_j^-$, and $\hat{\sigma}_i^-\hat{\sigma}_j^+$.

tweezers with programmable relative positions to the standing-wave cavity mode, leading to programmable atom cavity coupling strengths. Denoting the single-photon Rabi frequency at antinodes as $2g_0$, the coupling strength of the ith atom at position X_i is given by $2g_i = 2g_0 \sin(QX_i)$, with Q the cavity-mode wave vector. By manipulating the atom positions, we reach a programmable coupling $g_i = \lambda_i g_0$.

In order to realize the Raman coupling between $|\downarrow\rangle$ and $|\uparrow\rangle$, we send in two side coupling beams to off-resonantly couple $|\downarrow\rangle$ ($|\uparrow\rangle$) to $|e\rangle$ with frequencies ω_1 (ω_2) and Rabi frequencies Ω_1 (Ω_2), as shown in Fig. 1(b). The Hamiltonian $\hat{H}_{\rm exp}$ of such system is given by

$$\begin{aligned}\hat{H}_{\rm exp}/\hbar &= \omega\hat{a}^\dagger\hat{a} - \sum_{i=1}^{N}\{\omega_0|\downarrow\rangle_i\langle\downarrow| + (\omega_0-\Delta_F)|\uparrow\rangle_i\langle\uparrow|\} \\ &+ \sum_i\{\Omega_1\cos(\omega_1 t)|e\rangle_i\langle\downarrow| + \Omega_2\cos(\omega_2 t)|e\rangle_i\langle\uparrow| + \text{H.c.}\} \\ &+ \sum_i \lambda_i g_0\{\hat{a}|e\rangle_i\langle\downarrow| + \hat{a}|e\rangle_i\langle\uparrow| + \text{H.c.}\}, \end{aligned} \tag{2}$$

where $\hat{a}^\dagger$ ($\hat{a}$) is the creation (annihilation) operator of the cavity mode. Here, Δ_F is the hyperfine splitting between the two ground states $|\uparrow\rangle$ and $|\downarrow\rangle$, the energy zero point is set at the level of $|e\rangle$, ω is the cavity mode frequency, and ω_0 is the frequency of the transition $|\downarrow\rangle \to |e\rangle$. The detunings are organized as $\omega_1 = \omega_0 + \Delta + \Delta_F - \delta - \delta_m$, $\omega_2 = \omega_0 + \Delta - \Delta_F - \delta$, and $\omega = \omega_0 + \Delta$. The atom number N is equal to the number of integers (n) to divide for NPP.

After rotating wave approximation and adiabatically eliminating the excited state [32,33], each side coupling beam combined with the cavity mode forms a detuned Raman coupling between the two ground states, described by the Hamiltonian

$$\begin{aligned}\hat{H}'_{\rm exp}/\hbar \approx{}& \delta\hat{a}^\dagger\hat{a} + \tilde{\delta}_m\sum_i\hat{\sigma}_i^z \\ &+ \sum_i\lambda_i\{(g_{R,1}\hat{a} + g_{R,2}\hat{a}^\dagger)|\downarrow\rangle_i\langle\uparrow| + \text{H.c.}\}, \end{aligned} \tag{3}$$

where the two-photon couplings are given by $\lambda_i g_{R,1} = \Omega_1\lambda_i g_0/2(\Delta+\Delta_F)$ and $\lambda_i g_{R,2} = \Omega_2\lambda_i g_0/2\Delta$, respectively, $\hat{\sigma}^z$ is the Pauli-z operator, and $\tilde{\delta}_m$ describes the splitting between the ground states ac-Stark shifted by the coupling beams. By setting $\Omega_1/\Omega_2 = (\Delta+\Delta_F)/\Delta$, we achieve equal coupling strengths $g_{R,1} = g_{R,2} \equiv g_R$.

When $|g_R/\delta| \ll 1$, both two-photon processes are suppressed. The two Raman processes have opposite detunings $\pm\delta$ since one of them absorbs a cavity photon while the other emits one. Therefore, the four-photon process connecting two Raman couplings becomes resonant. As shown in Fig. 1(c), the total four processes realize the full $\lambda_i\lambda_j\hat{\sigma}_x^i\hat{\sigma}_x^j$ coupling. For example, at the leftmost of Fig. 1(c), a Raman process $\lambda_i g_{R,1}\hat{\sigma}_i^+\hat{a}^\dagger$ of the ith atom and a $\lambda_j g_{R,1}^*\hat{\sigma}_j^-\hat{a}$ process of the jth atom can form a resonant process $\lambda_i g_{R,1}\hat{\sigma}^+\lambda_j g_{R,1}^*\hat{\sigma}^-$. Even when the cavity is in vacuum states, the spins can still interact with each other via exchanging virtual photons through the cavity. Together with the other three similar processes that conserve the cavity photon number [see Fig. 1(c)], the system could realize the terms of $\hat{\sigma}_i^+\hat{\sigma}_j^+$, $\hat{\sigma}_i^-\hat{\sigma}_j^-$, $\hat{\sigma}_i^+\hat{\sigma}_j^-$, and $\hat{\sigma}_i^-\hat{\sigma}_j^+$. Since these four processes have equal coupling strengths, this leads to an effective Hamiltonian,

$$\hat{H}_{\rm eff}/\hbar = \sum_{i=1}^{N}\tilde{\delta}_m\hat{\sigma}_i^z + g_4\left(\sum_{i=1}^{N}\lambda_i\hat{\sigma}_i^x\right)^2. \tag{4}$$

Both $\tilde{\delta}_m$ and g_4 are dynamically tunable in experiments with constraints $|\Omega_{1,2}| \ll |\Delta|$, and $|g_R|, |\tilde{\delta}_m| \ll |\delta|$.

To reach the many-body ground state of $\hat{H}_{\rm NPP}$, we apply the AQC protocol in the following way. First, we begin with a finite detuning $\tilde{\delta}_m(t=0)$ and set $g_4(t=0) = 0$ by turning off the coupling beams Ω_1 and Ω_2. The ground state at this point is a trivial product state $|\downarrow\rangle^{\otimes n}$ that can be easily prepared by optical pumping with high fidelity. Then we adiabatically ramp the Hamiltonian following a path $s(t)$ that goes from zero to unity. That is, we control the detuning as $\tilde{\delta}_m(t) = [1-s(t)]\tilde{\delta}_m(0)$. Simultaneously, we ramp the intensity of the two incident lasers to the desired value as $\Omega_{1(2)}(t) = \sqrt{s(t)}\Omega_{1(2)}$, so that $g_4(t) = s(t)g_4$. Finally, the solution to the NPP problem is obtained by measuring the atomic spins in the Pauli-$\hat{\sigma}^x$ basis. There are several ways to improve the success probability of AQC, for example with optimizing the Hamiltonian path [10–13] or by iterative reverse annealing schemes [34–36].

For solving NPPs, besides our atom cavity proposal, there are also other candidate systems or protocols such as trapped ions [37], and Grover search in a central spin setup [38]. Our proposing atom cavity realization is expected to be more scalable for its convenience in increasing atom numbers. The theory we shall develop below may well be used to show all these systems have potential to solve generic quantum optimization with arbitrary connectivity. Nonetheless, we mainly consider the atom cavity system in this Letter.

Encoding for 3-SAT.—We consider a 3-SAT problem with n variables $x_1, \ldots, x_n$, and m clauses $f_1, \ldots, f_m$ [39]. The 3-SAT problem is defined by two $m \times 3$ matrices I and B, with

$$f_j = (x_{I_{j,1}} \oplus B_{j,1}) \vee (x_{I_{j,2}} \oplus B_{j,2}) \vee (x_{I_{j,3}} \oplus B_{j,3}), \tag{5}$$

where I contains integers from 1 to n, and B contains binary values. Solving 3-SAT has direct applications in computation technologies such as symbolic model checking [40],

automated theorem proving [41], and planning in artificial intelligence [42]. The idea is to map the 3-SAT problem to the atom cavity Hamiltonian in Eq. (1). We introduce

$$\begin{aligned} a_i &= \sqrt{\alpha_{m+i}} + \sum_{j:\, x_i \text{ in } f_j} \sqrt{\alpha_j} \\ b_i &= \sqrt{\alpha_{m+i}} + \sum_{j:\, \bar{x}_i \text{ in } f_j} \sqrt{\alpha_j}, \\ c_j &= d_j = \sqrt{\alpha_j}, \end{aligned} \tag{6}$$

with α_p the pth squarefree integer, starting from 1. Here, we have $i \in [1, n]$, and $j \in [1, m]$. The numbers $\{a_i\}$, $\{b_i\}$, $\{c_j\}$, and $\{d_j\}$ form a set $\mathcal{R}$, which contains $2n + 2m$ numbers, to be referred to as $r_k(I, B)$, with $k \in [1, 2n + 2m]$. Solving 3-SAT problem is equivalent to finding a subset of $\mathcal{R}$ with its numbers added up to a target,

$$T(n, m) = \sum_{i=1}^{n} \sqrt{\alpha_{m+i}} + 3 \sum_{j=1}^{m} \sqrt{\alpha_j}, \tag{7}$$

or more specifically solving $\sum_k y_k r_k(I, B) = T(n, m)$ with y_k taking binary values (0 or 1). This equivalence is guaranteed by the property of linear independence of radicals obeyed by the squarefree integers [32,43].

The 3-SAT problem now becomes optimizing

$$\min_{\{y_k\}} \left(\sum_k y_k r_k(I, B) - T(n, m) \right)^2, \tag{8}$$

which directly maps onto the atom cavity system [Eq. (1)]. The optimization here only involves local fields and interactions of the factorized form of $r_k r_{k'}$ as existent in the cavity system. The additional requirement for encoding 3-SAT compared to NPP is the control over Rabi frequency for each atom, which is feasible to the atom cavity system through local addressing for each atom.

The ground state $y_k^\star$ can be obtained by performing AQC. With our scheme, a 3-SAT with n variables and m clauses would cost $2n + 2m$ atoms. The corresponding atom number overhead in this encoding is

$$\text{Overhead} = n + 2m. \tag{9}$$

The 3-SAT solution is directly given by $x_i = y_i^\star$.

We remark here that vertex cover problems can also be encoded by the atom cavity system in a similar way as 3-SAT [32].

We also mention that in computation theory, an alternative approach has been developed to construct the equivalence between NPP and 3-SAT, by using a series of integer power of fours (4^p) [44], instead of squarefree integers. This would then require the atom couplings to grow exponentially with the atom number or to be exponentially precise, which is problematic for experimental implementation of large scale computation. This problem is absent in our construction using squarefree integers.

Encoding for QUBO.—QUBO is to minimize a quadratic objective function of binary variables with no constraints [45]. It corresponds to finding the ground state of an Ising model of n classical spins ($s_i = \pm$) on a graph [46],

$$E(\{s_i\}) = \sum_{i,i'>i} J_{ii'} s_i s_{i'}. \tag{10}$$

Mapping this Ising model on a physical system requires engineering nonlocal interactions, which is challenging to implement in experiments. Although the atom cavity system has long-range interactions [$\lambda_i \lambda_{i'}$ in Eq. (4)], their form does not necessarily match $J_{ii'}$. The number of free parameters in J scales quadratically with the number of Ising spins, whereas it scales linearly with the atom number for the interactions of the atom cavity system. This implies the minimal number of encoding atoms has to scale quadratically with n.

We now develop a protocol for mapping the QUBO problem to the atom cavity system. To proceed, we first adopt the parity encoding, introducing $b_{ii'} = s_i s_{i'}$ [47]. Treating (ii') as a one single site of a square lattice (with size $n \times n$), the interactions in J then become local fields, with a cost of introducing constraints $b_{ii'} b_{ii'+1} b_{i+1i'+1} b_{i+1i'} = 1$ [47]. The total number of these independent constraints is $(n-1)(n-2)/2$. We then rewrite the constraints in terms of 3-SAT formula

$$\begin{aligned} &(\beta \vee x_{ii'} \vee x_{ii'+1}) \wedge (\beta \vee \bar{x}_{ii'} \vee \bar{x}_{ii'+1}) \wedge (\beta \vee x_{i+1i'+1} \vee x_{i+1i'}) \\ &\wedge (\beta \vee \bar{x}_{i+1i'+1} \vee \bar{x}_{i+1i'}) \wedge (\bar{\beta} \vee \bar{x}_{ii'} \vee x_{ii'+1}) \\ &\wedge (\bar{\beta} \vee x_{ii'} \vee \bar{x}_{ii'+1}) \wedge (\bar{\beta} \vee \bar{x}_{i+1i'+1} \vee x_{i+1i'}) \\ &\wedge (\bar{\beta} \vee x_{i+1i'+1} \vee \bar{x}_{i+1i'}), \end{aligned} \tag{11}$$

with $x_{ii'} = (b_{ii'} + 1)/2$, and β an introduced auxiliary variable. Taking all constraints into account, we have a 3-SAT problem with $n' = (n-1)^2$ variables, and $m' = 4(n-1)(n-2)$ clauses. The corresponding defining matrices I_{const} and B_{const} are directly given according to Eqs. (5) and (11).

As shown above, the 3-SAT formulas are equivalent to the optimization problem in Eq. (8). Now, the QUBO problem becomes optimizing

$$\begin{aligned} \min \Bigg\{ &\sum_{k=1}^{n(n-1)/2} J_k y_k \\ &+ \mathcal{M} \left(\sum_{k=1}^{2(n'+m')} y_k r_k(I_{\text{const}}, B_{\text{const}}) - T(n', m') \right)^2 \Bigg\}, \end{aligned} \tag{12}$$

with the first $n(n-1)/2$ elements of y_k representing $x_{ii'}$, and J_k representing $J_{ii'}$ correspondingly. Here, energy

penalty term $\mathcal{M} > 0$ should be sufficiently large to enforce the required constraints. For practical AQC, it is suggested to start from a moderate $\mathcal{M}$, and check for convergence upon its increase.

Since the optimization in Eq. (12) only involves local fields and interactions of the factorized form of $r_k r_{k'}$, it maps directly to the atom cavity system. The solution of QUBO can be efficiently decoded from y_k using the algorithm developed for parity encoding [48]. The overhead in the cost of atom number for the QUBO problem is

$$\text{Overhead} = 2(n-1)(5n-9) - n. \tag{13}$$

The quadratic scaling of the overhead is already optimal. We thus have a universal atom cavity based quantum optimization solver for generic QUBO problem, with the scaling of the cost of atom numbers being optimal. We remark here that the atom cavity solver for QUBO problem does not require arranging the atoms in a regular two-dimensional array. Our scheme fully exploits the form of the nonlocal interactions of the cavity system.

Discussion.—We develop a universal quantum optimization architecture based on cold atoms in an optical cavity. A Raman scheme is constructed using four-photon processes, where the cavity photon induced atomic interactions naturally encode NPPs. We find 3-SAT and vertex cover problems can also be efficiently encoded by the atom cavity system, at a linear cost of atom number, which is in contrast to the quadratic overhead in the Rydberg encoding [15,16]. Based on the encoding scheme for 3-SAT, we further design an atom cavity architecture for generic QUBO problems with arbitrary connectivity. The atom number overhead for encoding QUBO has quadratic scaling, which is optimal for QUBO. We anticipate the atom cavity system to provide a compelling platform for quantum optimization having wide applications in academia and industry [49]. With our theory, the cavity system has a potential to become a universal quantum optimization platform to demonstrate practical quantum advantage. The decoherence of this system is mainly from the finite atomic excited state lifetime and the photon leakage, both of which are controllable by the two-photon detuning. Their tradeoff sets the limit of the quantum coherence time T. A worst-scenario estimate gives $g_4 T \propto \eta^{1/2}/N$, with η the cavity cooperativity [32]. The quantum coherence can be further improved by considering more advanced techniques such as cross cavities, by which we have $g_4 T \propto \eta^{3/2}$ in the large atom number limit. This implies that our scheme is scalable, and that the coherence time can be systematically improved by advancing the cavity engineering technology.

We acknowledge helpful discussion with Changling Zou and Lei Shi. This work is supported by National Key Research and Development Program of China (2021YFA1400900 and 2021YFA0718303), National Natural Science Foundation of China (11934002, 92165203, 61975092, and 11974202), and Shanghai Municipal Science and Technology Major Project (Grant No. 2019SHZDZX01).

*zhangwenjun@ultracold.group
†cwlaser@ultracold.cn
‡xiaopengli@fudan.edu.cn
§These authors contributed equally to this work.

[1] E. Farhi, J. Goldstone, S. Gutmann, J. Lapan, A. Lundgren, and D. Preda, Science **292**, 472 (2001).
[2] E. Farhi, J. Goldstone, and S. Gutmann, arXiv:1411.4028.
[3] A. Perdomo-Ortiz, N. Dickson, M. Drew-Brook, G. Rose, and A. Aspuru-Guzik, Sci. Rep. **2**, 571 (2012).
[4] I. Gaidai, D. Babikov, A. Teplukhin, B. K. Kendrick, S. M. Mniszewski, Y. Zhang, S. Tretiak, and P. A. Dub, Sci. Rep. **12**, 16824 (2022).
[5] B. N. Clark, C. J. Colbourn, and D. S. Johnson, Discrete Math. **86**, 165 (1990).
[6] L. Zhou, S.-T. Wang, S. Choi, H. Pichler, and M. D. Lukin, Phys. Rev. X **10**, 021067 (2020).
[7] M. B. Hastings, Quantum **5**, 597 (2021).
[8] S. Ebadi *et al.*, Science **376**, 1209 (2022).
[9] A. D. King *et al.*, Nature (London) **617**, 61 (2023).
[10] J. Lin, Z. Y. Lai, and X. Li, Phys. Rev. A **101**, 052327 (2020).
[11] J. Lin, Z. Zhang, J. Zhang, and X. Li, Phys. Rev. A **105**, 062455 (2022).
[12] B. F. Schiffer, J. Tura, and J. I. Cirac, PRX Quantum **3**, 020347 (2022).
[13] Y.-Q. Chen, Y. Chen, C.-K. Lee, S. Zhang, and C.-Y. Hsieh, Nat. Mach. Intell. **4**, 269 (2022).
[14] A. Browaeys and T. Lahaye, Nat. Phys. **16**, 132 (2020).
[15] X. Qiu, P. Zoller, and X. Li, PRX Quantum **1**, 020311 (2020).
[16] M.-T. Nguyen, J.-G. Liu, J. Wurtz, M. D. Lukin, S.-T. Wang, and H. Pichler, PRX Quantum **4**, 010316 (2023).
[17] P. Scholl, M. Schuler, H. J. Williams, A. A. Eberharter, D. Barredo, K.-N. Schymik, V. Lienhard, L.-P. Henry, T. C. Lang, T. Lahaye, A. M. Läuchli, and A. Browaeys, Nature (London) **595**, 233 (2021).
[18] S. Ebadi, T. T. Wang, H. Levine, A. Keesling, G. Semeghini, A. Omran, D. Bluvstein, R. Samajdar, H. Pichler, W. W. Ho, S. Choi, S. Sachdev, M. Greiner, V. Vuletić, and M. D. Lukin, Nature (London) **595**, 227 (2021).
[19] M. Kim, K. Kim, J. Hwang, E.-G. Moon, and J. Ahn, Nat. Phys. **18**, 755 (2022).
[20] T. M. Graham *et al.*, Nature (London) **604**, 457 (2022).
[21] C. Sheng, J. Hou, X. He, K. Wang, R. Guo, J. Zhuang, B. Mamat, P. Xu, M. Liu, J. Wang, and M. Zhan, Phys. Rev. Lett. **128**, 083202 (2022).
[22] M. Saffman, T. G. Walker, and K. Mølmer, Rev. Mod. Phys. **82**, 2313 (2010).
[23] C. L. Degen, F. Reinhard, and P. Cappellaro, Rev. Mod. Phys. **89**, 035002 (2017).
[24] H. Ritsch, P. Domokos, F. Brennecke, and T. Esslinger, Rev. Mod. Phys. **85**, 553 (2013).
[25] A. Reiserer and G. Rempe, Rev. Mod. Phys. **87**, 1379 (2015).

[26] A. Blais, A. L. Grimsmo, S. M. Girvin, and A. Wallraff, Rev. Mod. Phys. **93**, 025005 (2021).
[27] E. J. Davis, G. Bentsen, L. Homeier, T. Li, and M. H. Schleier-Smith, Phys. Rev. Lett. **122**, 010405 (2019).
[28] J. A. Muniz, D. Barberena, R. J. Lewis-Swan, D. J. Young, J. R. K. Cline, A. M. Rey, and J. K. Thompson, Nature (London) **580**, 602 (2020).
[29] A. Periwal, E. S. Cooper, P. Kunkel, J. F. Wienand, E. J. Davis, and M. Schleier-Smith, Nature (London) **600**, 630 (2021).
[30] Y. Liu, Z. Wang, P. Yang, Q. Wang, Q. Fan, S. Guan, G. Li, P. Zhang, and T. Zhang, Phys. Rev. Lett. **130**, 173601 (2023).
[31] L. Coslovich, R. Pesenti, and W. Ukovich, Ukio Technologinis ir Ekonominis Vystymas **12**, 18 (2006).
[32] See Supplemental Material at http://link.aps.org/supplemental/10.1103/PhysRevLett.131.103601 for technical details for the atom-cavity system and the encoding protocol.
[33] H. Tanji-Suzuki, I. D. Leroux, M. H. Schleier-Smith, M. Cetina, A. T. Grier, J. Simon, and V. Vuletić, in *Advances in Atomic, Molecular, and Optical Physics* edited by E. Arimondo, P. R. Berman, and C. C. Lin (Academic Press, New York, 2011), Vol. 60, pp. 201–237, ISSN: 1049-250X.
[34] A. Perdomo-Ortiz, S. E. Venegas-Andraca, and A. Aspuru-Guzik, Quantum Inf. Process. **10**, 33 (2011).
[35] N. Chancellor, New J. Phys. **19**, 023024 (2017).
[36] Y. Yamashiro, M. Ohkuwa, H. Nishimori, and D. A. Lidar, Phys. Rev. A **100**, 052321 (2019).
[37] T. Graß, D. Raventós, B. Juliá-Díaz, C. Gogolin, and M. Lewenstein, Nat. Commun. **7**, 11524 (2016).
[38] G. Anikeeva, O. Marković, V. Borish, J. A. Hines, S. V. Rajagopal, E. S. Cooper, A. Periwal, A. Safavi-Naeini, E. J. Davis, and M. Schleier-Smith, PRX Quantum **2**, 020319 (2021).
[39] M. V. A. Yu Kitaev and A. H. Shen, *Classical and Quantum Computation* (American Mathematical Society, Providence, 2000), Vol. 47.
[40] K. L. McMillan, in *Computer Aided Verification: 15th International Conference, CAV 2003, Boulder, CO, USA, 2003. Proceedings 15* (Springer, New York, 2003), pp. 1–13.
[41] T. H. Cormen, C. E. Leiserson, R. L. Rivest, and C. Stein, *Introduction to Algorithms* (MIT Press, Cambridge, MA, 2022).
[42] H. Kautz and B. Selman, in *IJCAI* (Morgan Kaufmann Publishers Inc., San Francisco, 1999), Vol. 99, pp. 318–325.
[43] S. Shah, T. LAM, and D. ROWLAND, the Harvard College Mathematics Review (2007), https://abel.math.harvard.edu/hcmr/issues/2.pdf.
[44] T. H. Cormen, C. E. Leiserson, R. L. Rivest, and C. Stein, *Introduction to Algorithms* (MIT Press, Cambridge, MA, 2022).
[45] G. Kochenberger, J.-K. Hao, F. Glover, M. Lewis, Z. Lü, H. Wang, and Y. Wang, J. Comb. Optim. **28**, 58 (2014).
[46] G. E. Santoro, R. Martoňák, E. Tosatti, and R. Car, Science **295**, 2427 (2002).
[47] W. Lechner, P. Hauke, and P. Zoller, Sci. Adv. **1**, e1500838 (2015).
[48] F. Pastawski and J. Preskill, Phys. Rev. A **93**, 052325 (2016).
[49] P. Hauke, H. G. Katzgraber, W. Lechner, H. Nishimori, and W. D. Oliver, Rep. Prog. Phys. **83**, 054401 (2020).